Chiral condensate in $n_f = 2$ QCD from the Banks–Casher relation

Georg P. Engel[*]

Dipartimento di Fisica, Università Milano-Bicocca,
and INFN, Sezione di Milano-Bicocca,
Piazza della Scienza 3, 20126 Milano, Italy
E-mail: `georg.engel@mib.infn.it`

Exploiting the Banks-Casher relation, we present a direct determination of the chiral condensate in two-flavor QCD, computing the mode number of the $\mathcal{O}(a)$-improved Wilson-Dirac operator below various cutoffs. We make use of CLS-configurations with three different lattice spacings in the range of 0.05-0.08 fm and pion masses down to 190 MeV. Our data indicate a non-zero density of eigenmodes near the origin and hence points to spontaneous chiral symmetry breaking. We extrapolate our results to the continuum and chiral limit to give a result for the chiral condensate.

---

[*]Speaker.

1. Introduction

The chiral condensate, defined as expectation value of a quark-antiquark pair,

$$\Sigma \equiv -\frac{1}{2}\langle \bar{\psi}\psi \rangle \,, \tag{1.1}$$

plays a central rôle in QCD. It provides an order parameter for chiral symmetry breaking, a leading-order low-energy constant of Chiral Perturbation Theory (ChPT), and it naturally appears in the Operator Product Expansion. Recent related lattice QCD results are collected in the FLAG review [1]. The present work discusses a determination of Σ, exploiting the Banks-Casher relation [2],

$$\Sigma = \pi \lim_{\lambda \to 0} \lim_{m \to 0} \lim_{V \to \infty} \rho(\lambda, m) \,, \tag{1.2}$$

$$\text{with} \qquad \rho(\lambda, m) = \frac{1}{V} \sum_{k=1}^{\infty} \langle \delta(\lambda - \lambda_k) \rangle \,, \tag{1.3}$$

where m is the current quark mass, $i\lambda_k$ are the eigenvalues of the massless Dirac operator and V is the four-volume. The spectral density ρ is renormalizable and can be computed on the lattice numerically [3]. In lattice QCD with Wilson-type quarks, it turns out to be convenient to consider the mode number $\nu(\Lambda, m)$ of the massive hermitian operator $D_m^\dagger D_m$ with eigenvalues $\alpha \leq M = \sqrt{\Lambda^2 + m^2}$, which is renormalization-group invariant,

$$\nu(\Lambda, m) = V \int_{-\Lambda}^{\Lambda} d\lambda \rho(\lambda, m) \tag{1.4}$$

$$\nu_R(\Lambda_R, m_R) = \nu(\Lambda, m) \,. \tag{1.5}$$

The method was shown to work in Ref. [3] and applied to twisted–mass fermions in Ref. [4]. We define the effective spectral density,

$$\tilde{\rho}_R = \frac{\pi}{2V} \frac{\nu_{2,R} - \nu_{1,R}}{\Lambda_{2,R} - \Lambda_{1,R}} \,, \tag{1.6}$$

which agrees with Σ after taking the appropriate order of limits as in the Banks-Casher relation. Note that any threshold effects are removed from $\tilde{\rho}_R$ as long as all $\Lambda_{i,R}$ are chosen large enough. Preliminary results have been presented in Ref. [5], the main physics results are published in Ref. [6], while for a detailed discussion we refer to Ref. [7].

2. Chiral Perturbation Theory

At next-to-leading-order (NLO), continuum ChPT predicts for $n_f = 2$ QCD [3],

$$\tilde{\rho}_R^{\text{NLO}}(\Lambda_{1,R}, \Lambda_{2,R}, m_R) = \Sigma \left\{ 1 + \frac{m_R \Sigma}{(4\pi)^2 F^4} \left[3\bar{l}_6 + 1 - \ln(2) - 3\ln\left(\frac{\Sigma m_R}{F^2 \mu^2}\right) + \tilde{g}_\nu\left(\frac{\Lambda_{1,R}}{m_R}, \frac{\Lambda_{2,R}}{m_R}\right) \right] \right\} \,, \tag{2.1}$$

where $\tilde{g}_\nu(x_1, x_2)$, explicitly given in Ref. [5], appears to be a mild function in the considered range of parameters [7]. F is the pseudo-scalar decay constant in the chiral limit, $\bar{l}_6$ an NLO low-energy constant (LEC) and μ is a fixed scale. It is noteworthy that there are no chiral logarithms at fixed

id	L/a	m_π [MeV]	$m_\pi L$	a [fm]	$R\tau_{\rm exp}$	$R\tau_{\rm int}(m_\pi)$	$R\tau_{\rm int}(\nu)$	$Rn_{\rm it}(\nu)$	$N_{\rm cnfg}$
A3	32	496(6)	6.0	0.0749(8)	40	7		47.36	55
A4		386(5)	4.7			5		53.28	55
A5		333(5)	4.0			5	3	36.00	55
B6	48	283(4)	5.2			6		24.00	50
E5	32	440(5)	4.7	0.0652(6)	55	9	6	35.52	92
F6	48	314(3)	5.0			8		29.60	50
F7		268(3)	4.3			7		26.64	50
G8	64	193(2)	4.1			8		24-48	50
N5	48	443(4)	5.2	0.0483(4)	100	30	11	28.16	60
N6		342(3)	4.0			10		128.0	60
O7	64	269(3)	4.2			15		76.00	50

Table 1: Parameters of the simulation. L is the linear spatial extent of the lattice, a the lattice spacing [12], m_π the pion mass, R the ratio of active links in DD-HMC [13] ($R = 1$ in MP-HMC [14]). $\tau_{\rm exp}$ and $\tau_{\rm int}$ denote the exponential and integrated autocorrelation time, resp., given in units of molecular dynamics, $n_{\rm it}$ the separation of configurations between subsequent measurements and $N_{\rm cnfg}$ the number of configurations on which ν is measured.

$\Lambda_{\rm R}$, that $\tilde\rho_{\rm R}^{\rm NLO}$ is a decreasing function of $\Lambda_{\rm R} = (\Lambda_{1,{\rm R}} + \Lambda_{2,{\rm R}})/2$ for any finite quark mass, and also that in the chiral limit all NLO-corrections vanish in the two-flavor theory [3, 8].

NLO Wilson-ChPT, considering $\mathcal{O}(a)$ improvement and the generically-small-quark-mass regime (GSM) [9], gives an additional term of the form $m_{\rm R}/(\Lambda_{1,{\rm R}}\Lambda_{2,{\rm R}})$ added to Eq. (2.1). The sign of this term was argued to be positive [10, 11], which implies that $\tilde\rho_{\rm R}^{\rm NLO,lat}$ is a decreasing function of $\Lambda_{\rm R}$ also at finite lattice spacing (in the GSM-regime). We remark that those NLO discretization effects, and any $\Lambda_{\rm R}$-dependence, are still absent in the chiral limit. The formalism of ChPT can be used also to address finite-volume effects, which increase towards light $\Lambda_{\rm R}$.

3. Details of the simulation

We measure the mode number on configurations with two flavors of $\mathcal{O}(a)$-improved Wilson quarks, provided by the CLS-collaboration. The most relevant details for the present study are depicted in Tab. 1, further information is detailed in Refs. [12, 15]. Finite-size effects and autocorrelations are under control for all measurements. The mode number is computed for nine values of $\Lambda_{\rm R}$ in the range 20-120 MeV with a statistical precision of a few percent on all ensembles. Rational polynomials are used to approximate the the spectral projector $\mathbb{P}_M$ to the low modes of the Dirac operator. Its expectation value is then evaluated stochastically with pseudo-fermion fields η_k,

$$\nu = \frac{1}{N}\sum_{k=1}^{N}\langle(\eta_k, \mathbb{P}_M\eta_k)\rangle, \qquad M = \sqrt{\Lambda^2 + m^2}. \tag{3.1}$$

4. Results

Fig. 1, left, shows the results for the mode number for all ensembles. It exhibits a roughly linear dependence on aM in all cases up to approximately 100-150 MeV. A phenomenological low-order

polynomial fit indicates that in the considered range roughly 90% of v is given by the linear term. The effective spectral density $\tilde{\rho}_R$ shows a non-zero and flat behavior in Λ_R at fine lattice spacings and light quark masses. As an example, the results of ensemble O7 are shown in Fig. 1, right.

To extrapolate to the continuum and chiral limit, some analytic guidance is needed. In this respect, first studies indicated that higher-order effects of ChPT are apparent in the data and correspondingly the functional form at finite lattice spacing is not entirely clear in the considered range of parameters [5]. For this reason, we attempt to build a clean fitting strategy where different effects can be distinguished clearly. Such a strategy is based on performing first the continuum limit, and only then removing the small corrections stemming from finite m_R and Λ_R. To do so, we interpolate $\tilde{\rho}_R$ to three values of the quark mass ($m_R = 12.9, 20.9, 32.0$ MeV) at each lattice spacing. A continuum extrapolation is then performed separately for each pair of (Λ_R, m_R), examples of which are shown in Fig. 2. The linear a^2-dependence, expected from Symanzik effective theory for the $\mathscr{O}(a)$-improved theory, is respected well by the data. It is noteworthy that the discretization effects exhibit a non-trivial dependence on (Λ_R, m_R), but appear fairly mild at the lightest points.

As a result of the extrapolation, we obtain $\tilde{\rho}_R$ in the continuum, where its non-zero values at light (Λ_R, m_R) point to dynamical chiral symmetry breaking. This motivates to use ChPT to remove the remaining small corrections. We consider a fit function based on generalized NLO ChPT,

$$\tilde{\rho}_R = c_0(\Lambda_R) + c_1 m_R + c_2 m_R \left[\tilde{g}_v \left(\frac{\Lambda_{1,R}}{m_R}, \frac{\Lambda_{2,R}}{m_R} \right) - 3 \ln \left(\frac{m_R}{\mu} \right) \right] , \qquad (4.1)$$

where $c_0(\Lambda_R) = \Sigma = $ const. at NLO. The continuum data is described well by this ansatz (the correlated fit gives $\chi^2/$dof=16.4/14), the extrapolation is of the order of the statistical error, and we obtain the results for $c_0(\Lambda_R)$ shown in Fig. 3. The plateau-like behavior for $\Lambda_R \leq 80$ MeV indicates the NLO range, and a corresponding fit gives $\Sigma^{1/3} = 261(6)$ MeV in the $\overline{\text{MS}}$ scheme at 2 GeV.

To substantiate the result, we consider a second strategy to extract the chiral condensate from the data on the effective spectral density. After the separate treatment of different effects in the first strategy, we now attempt to perform a combined fit in (Λ_R, m_R, a) at once. The advantages are that this approach does not require an interpolation in m_R but includes all data, and furthermore needs fewer fit parameters compared to the first strategy. However, ChPT is used from the start and the discretization effects have to be modelled. We assume a linear dependence in a^2 and m_R, but still allow for an arbitrary Λ_R-dependence, inspired by Symanzik effective theory and the chiral power expansion. It is worth noting that the model complies with the results of the first strategy and includes NLO Wilson-ChPT [9] as a special case. We find that the fit describes the data well and that the results agree very well with the ones of the first strategy. Having abundant degrees of freedom in the fit, we use the second strategy to estimate the systematic uncertainty of the final result by performing various different fits. An upward shift is found when neglecting data at coarse lattices, while a downward shift is found when including higher-order terms $\mathscr{O}(\Lambda_R^2, m_R^2)$ in the fit.

5. Conclusions

We presented a determination of the chiral condensate based on an extensive discussion of the spectral density of the hermitean Wilson Dirac operator. Our final result is

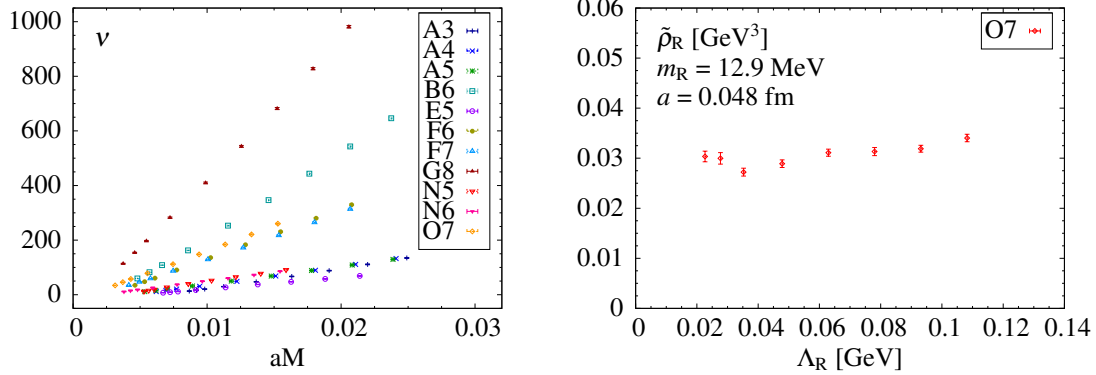$$[\Sigma^{\overline{\text{MS}}}(2 \text{ GeV})]^{1/3} = 261(6)(8) \text{ MeV} , \qquad (5.1)$$

Figure 1: First look at the numerical data. Left: Mode number ν for all ensembles vs. the bare dimensionless cutoff aM. Note the approximate linearity and the high number of modes achieved for small quark masses. Right: Effective spectral density $\tilde{\rho}_R$ vs. the cutoff Λ_R for the ensemble with the lightest quark mass at the finest lattice spacing (O7). Note the non-zero flat behavior, which can be interpreted as a first hint for dynamical chiral symmetry breaking.
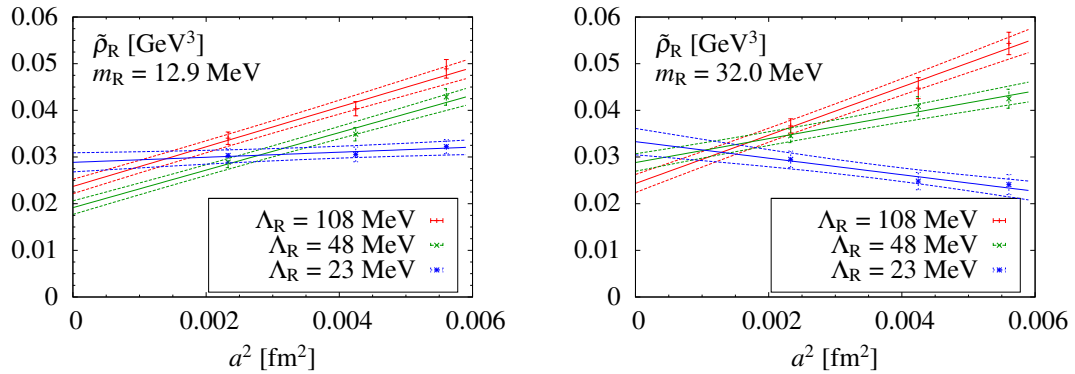

Figure 2: Continuum extrapolation of $\tilde{\rho}_R$, performed individually for each pair (Λ_R, m_R). Shown for three values of Λ_R covering the entire range, and for the lightest (left) and the heaviest reference quark mass (right). Note that the data agrees well with the linear a^2-dependence expected in the $\mathcal{O}(a)$-improved theory. The discretization effects exhibit a non-trivial dependence on (Λ_R, m_R), but appear mild at the lightest point.

where the first error is statistical and the second one systematic. As a consistency test of dynamical symmetry breaking and ChPT, we consider its NLO prediction for the quark mass dependence of the pion mass. The latter is known as GMOR-relation and we show its prediction based on our measurement of the chiral condensate together with the direct measurements of the quark and pion masses in Fig. 4. The relation appears to be fulfilled to very good precision in the range considered.
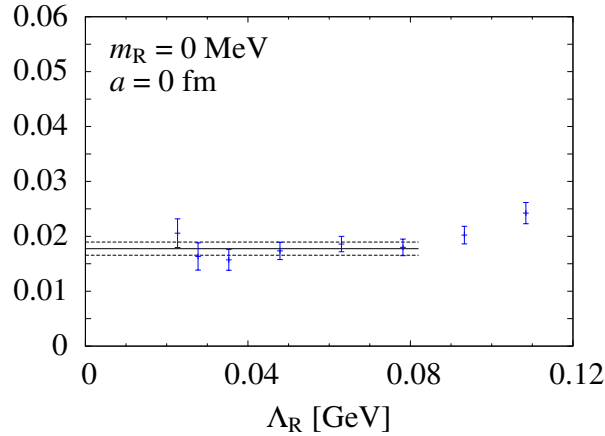
Acknowledgments

Figure 3: The effective spectral density $\tilde{\rho}_R$ in the continuum and chiral limit. The flat and non-zero behavior observed for $\Lambda \leq 80$ MeV is consistent with NLO ChPT, a plateau fit in this range yields a prediction for the chiral condensate given in the text.
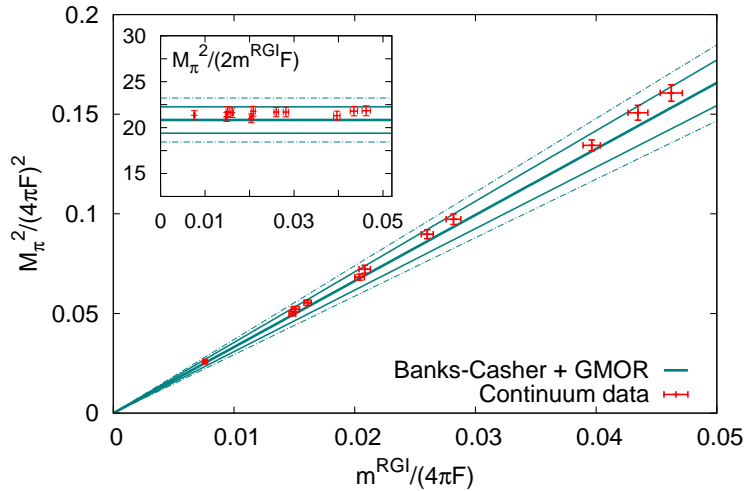

Figure 4: Consistency of the determined chiral condensate with the quark mass dependence of the pion mass as expected from the GMOR-relation. The pion mass squared M_π^2 is shown vs. the renormalization-group-independent (RGI) quark mass, normalized to $4\pi F$ (≈ 1 GeV), where F is the pseudo-scalar decay constant in the chiral limit (taken from [6]). The direct measurements (red symbols) are extrapolated to the continuum as described in Ref. [6], while the (central) solid line represents the GMOR contribution to the pion mass squared, computed by taking the direct determination of the chiral condensate through the spectral density. The thinner solid lines denote the statistical error, the dotted-dashed ones the sum of statistical and systematic one.

and the technical support. We are grateful to our colleagues within the CLS initiative for sharing the ensembles of gauge configurations. We acknowledge partial support by the MIUR-PRIN contract 20093BMNNPR.

References

[1] S. Aoki, Y. Aoki, C. Bernard, T. Blum, G. Colangelo, *et. al.*, *Review of lattice results concerning low energy particle physics*, `arXiv:1310.8555`.

[2] T. Banks and A. Casher, *Chiral Symmetry Breaking in Confining Theories*, *Nucl.Phys.* **B169** (1980) 103.

[3] L. Giusti and M. Lüscher, *Chiral symmetry breaking and the Banks-Casher relation in lattice QCD with Wilson quarks*, *JHEP* **0903** (2009) 013, [`arXiv:0812.3638`].

[4] K. Cichy, E. Garcia-Ramos, and K. Jansen, *Chiral condensate from the twisted mass Dirac operator spectrum*, *PoS* **LATTICE2013** (2013) 128, [`arXiv:1303.1954`].

[5] G. P. Engel, L. Giusti, S. Lottini, and R. Sommer, *Chiral condensate from the Banks-Casher relation*, *PoS* **LATTICE2013** (2013) 119, [`arXiv:1309.4537`].

[6] G. P. Engel, L. Giusti, S. Lottini, and R. Sommer, *Chiral symmetry breaking in QCD Lite*, `arXiv:1406.4987`.

[7] G. P. Engel, L. Giusti, S. Lottini, and R. Sommer, *Spectral density of the Dirac operator in two-flavour QCD*, `arXiv:1411.6386`.

[8] A. V. Smilga and J. Stern, *On the spectral density of Euclidean Dirac operator in QCD*, *Phys.Lett.* **B318** (1993) 531–536.

[9] S. Necco and A. Shindler, *Spectral density of the Hermitean Wilson Dirac operator: a NLO computation in chiral perturbation theory*, *JHEP* **1104** (2011) 031, [`arXiv:1101.1778`].

[10] M. T. Hansen and S. R. Sharpe, *Constraint on the Low Energy Constants of Wilson Chiral Perturbation Theory*, *Phys.Rev.* **D85** (2012) 014503, [`arXiv:1111.2404`].

[11] K. Splittorff and J. Verbaarschot, *The Microscopic Twisted Mass Dirac Spectrum*, *Phys.Rev.* **D85** (2012) 105008, [`arXiv:1201.1361`].

[12] P. Fritzsch, F. Knechtli, B. Leder, M. Marinkovic, S. Schaefer, *et. al.*, *The strange quark mass and Lambda parameter of two flavor QCD*, *Nucl.Phys.* **B865** (2012) 397–429, [`arXiv:1205.5380`].

[13] M. Lüscher, *Solution of the Dirac equation in lattice QCD using a domain decomposition method*, *Comput.Phys.Commun.* **156** (2004) 209–220, [`hep-lat/0310048`].

[14] M. Marinkovic and S. Schaefer, *Comparison of the mass preconditioned HMC and the DD-HMC algorithm for two-flavour QCD*, *PoS* **LATTICE2010** (2010) 031, [`arXiv:1011.0911`].

[15] M. Marinkovic, S. Schaefer, R. Sommer, and F. Virotta, *Strange quark mass and Lambda parameter by the ALPHA collaboration*, *PoS* **LATTICE2011** (2011) 232, [`arXiv:1112.4163`].